

1 **Rain concentration and sheltering effect of solar panels on cultivated plots**

2

3 Yassin Elamri^{1,2}, Bruno Cheviron³, Annabelle Mange⁴, Cyril Dejean⁵, François Liron⁶, Gilles Belaud⁷

4

5 ¹ UMR G-Eau, Irstea, Univ. Montpellier, 361 rue Jean-François Breton 34136 Montpellier (FRANCE),

6 *yassin.elamri@irstea.fr*

7 ² Sun'R sas, 41 quai Fulchiron 69005 Lyon (FRANCE), *yassin.elamri@sunr.fr*

8 ³ UMR G-Eau, Irstea, Univ. Montpellier, 361 rue Jean-François Breton 34136 Montpellier (FRANCE),

9 *bruno.cheviron@irstea.fr*

10 ⁴ UMR G-Eau Irstea, Univ. Montpellier,, 361 rue Jean-François Breton 34136 Montpellier (FRANCE),

11 *annabelle.mange@irstea.fr*

12 ⁵ UMR G-Eau, Irstea, Univ. Montpellier, 361 rue Jean-François Breton 34136 Montpellier (FRANCE),

13 *cyril.dejean@irstea.fr*

14 ⁶ UMR G-Eau, Irstea, Univ. Montpellier, 361 rue Jean-François Breton 34136 Montpellier (FRANCE),

15 *francois.liron@irstea.fr*

16 ⁷ UMR G-Eau, Montpellier Supagro, Univ. Montpellier, 2 place Pierre Viala 34060 Montpellier (FRANCE),

17 *gilles.belaud@supagro.fr*

18

19 **Abstract**

20

21 Agrivoltaism is the association of agricultural and photovoltaic energy production on the same land
22 area, coping with the increasing pressure on land use and water resources while delivering a clean
23 and renewable energy. However the solar panels located above the cultivated plots also have a
24 seemingly unexplored yet effect on rain redistribution, sheltering large parts of the plot but
25 redirecting concentrated fluxes on a few locations. The spatial heterogeneity in water amounts
26 observed on the ground is high in the general case; its dynamical patterns are directly attributable to
27 the mobile panels through their geometrical characteristics (dimensions, height, coverage
28 percentage) and the strategies selected to rotate them around their support tube. A coefficient of
29 variation is used to measure this spatial heterogeneity and to compare it with the coefficient of
30 uniformity that classically describes the efficiency of irrigation systems. A rain redistribution model
31 (AVrain) was derived from literature elements and theoretical grounds then validated from
32 experiments in both field and controlled conditions. AVrain simulates the effective rain amounts on
33 the plot from a few forcing data (rainfall, wind velocity and direction) thus allows real-time strategies
34 that consist in operating the panels so as to limit rain interception mainly responsible for the spatial
35 heterogeneities. Such avoidance strategies resulted in a sharp decrease of the coefficient of
36 variation, e.g. 0.22 against 2.13 for panels held flat during one of the monitored rain events, that is a
37 fairly good uniformity score for irrigation specialists. Finally, the water amounts predicted by AVrain
38 were used as inputs to HYDRUS-2D for a brief exploratory study on the impact of the presence of
39 solar panels on rain redistribution at shallow depths within soils; similar, more diffuse patterns were
40 simulated and coherent with field measurements.

Supprimé:

Supprimé:

41

42 **Copyright statement**

43

44 Data collection and model development were performed in the frame of the Sun'Agri2B project that
45 links the Sun'R SAS society with Irstea, SupAgro Montpellier and other academic or non-academic
46 partners. The copyright on all experimental and theoretical results presented here is governed by the
47 consortium agreement of the Sun'Agri2B project.

48

51 **1. Introduction**

52 The current climate change context induced by the production and consumption of highly polluting
53 fossil energies, responsible for the greenhouse effect, has in turn triggered the development of clean
54 and renewable energies with special interest for photovoltaic systems (IPCC, 2014). The recent times
55 have seen a clear increase of land coverage by solar panels disposed on roofs, used for parking
56 shadehouses or organized in solar farms (IPCC, 2011). In the last years, solar panels were installed
57 above cultivated plots in France (Marrou, 2012), in Japan (Movellan, 2013), in India (Harinarayana
58 and Vasavi, 2014), in the USA (Ravi et al., 2014) and in Germany (Osborne, 2016) so as not to create
59 competition between different land uses (Dinesh and Pearce 2016). These innovative devices termed
60 "agrivoltaic" by Dupraz et al. (2011) allow maintaining the agricultural yield under certain conditions
61 (Marrou et al., 2013b; Marrou et al., 2013c), together with water savings (Marrou et al., 2013a)
62 which results in the expected higher values of the dedicated "land use efficiency" indicator (Marrou
63 2012)

64
65 Besides blocking and converting a part of the incoming solar radiation, the implementation of solar
66 panels in natural settings has a series of direct or indirect effects on several terms of the hydrological
67 budget, in the equipped plots (Cook and McCuen 2013; Barnard et al. 2017). Although far less
68 studied, these on-site or off-site hydrological consequences should be addressed and modeled for
69 site preservation purposes in the general case and also because they are very likely to constrain the
70 optimal irrigation and local site management strategies, on the cultivated plots. For example,
71 Diermanse (1999) showed that a correct simulation of runoff could often be achieved at the
72 watershed scale from spatially-averaged rainfall values, although clearly better results may be
73 expected when explicitly accounting for the subscale spatial patterns of rain distribution (Faurès et
74 al., 1995; Tang et al., 2007; Emmanuel et al., 2015). At the plot scale, rain interception and
75 redistribution by the crops (Levia and Germer, 2015; Yuan et al., 2017) is already known to cause
76 strong spatial heterogeneities (through stemflow, throughfall or improved water storage capabilities)
77 thus to raise multiple questions on soil microbiology, non-point source pollution and irrigation
78 piloting (Lamm and Manges, 2000; Martello et al., 2015). The presence of solar panels will provide
79 similar, additional issues, close to these experienced in agroforestry when the vegetative cover is of
80 various heights and nature, with a direct impact on the spatiotemporal patterns of rain redistribution
81 (Jackson, 2000). More into details and more specifically, the interception of rain by the impervious
82 surface of the solar panels produces an "umbrella effect" that delineates a sheltered area. By
83 contrast, its contour receives the collected fluxes, whose intensity or amounts may locally exceed
84 these of the control conditions, depending on the dimensions, height and tilting angle of the panels

85 as well as on wind velocity and direction. Cook and McCuen (2013) stated that one benefit of grass
86 growing was to damp or suppress any specific effect of solar panels on runoff at the plot scale. This
87 also constitutes valuable preventive measure against erosion issues arising from concentrated flows
88 in micro-gullies (Knapen et al., 2007; Gumiere et al., 2009) or attributable to the direct mechanical
89 effects of droplet impacts, known as splash erosion (Nearing and Bradford, 1985; Josserand and
90 Zaleski, 2003).

91

92 Agricultural soils should preferentially not be left bare under solar panel structures, because of
93 increased risks of runoff and erosion but these are only the most severe particular cases among the
94 diverse rain redistribution effects investigated in the present paper. These are possibly described
95 from geometrical arguments for an intuitive overview, suggesting three categories of zones on the
96 ground, in the agrivoltaic plots, (i) the non-impacted zones between panels that receive the same
97 rain amounts as the control site, (ii) the sheltered zones located right under the panels that receive
98 far less rainfall than in the control conditions and (iii) the border zones located where panels
99 discharge the collected rain amounts.

100

101 In most cultivated plots, the spatial heterogeneity of rainfall is limited before that of the other
102 determinants of the water budget and crop yield, typically the lateral and vertical variations of soil
103 properties and the non-uniformity of irrigation. Conversely, the presence of solar panels may cause
104 strong spatial heterogeneities possibly compared to that of the water abduction systems used for
105 irrigation, whose efficiency is estimated from the values of a coefficient of uniformity (Burt et al.,
106 1997; Playán and Mateos, 2006; Pereira et al., 2002). This paper therefore aims at characterizing the
107 effective rain distribution in agrivoltaic plots from the calculation of discharge volumes at the outlet
108 of the panels, depending on their tilting angle. Moreover, the procedure applies to mobile panels
109 endowed with one degree of freedom, i.e. able to rotate around their support tube according to
110 predefined strategies, which defines and introduces "dynamic agrivoltaism". Water redistribution in
111 soils comes in accordance and is briefly described here for coherence checks, it is not the main scope
112 of the manuscript though crucial for crop growth and irrigation optimisation.

113

114 Sect. 2 describes the experimentations conducted on the agrivoltaic plot (Sect. 2.1) and in controlled
115 conditions (Sect. 2.2), also presenting the AVrain model that predicts rain redistribution by the solar
116 panels (Sect. 2.3). Sect. 3 shows the experimental and modelling results, discussed in Sect. 4. Sect. 5
117 gathers the conclusions and openings of this work.

118

Supprimé: weak

120 **2. Material and methods**

121 *2.1. Field experiments*

122 **2.1.1. Agrivoltaic plot**

123 The agrivoltaic plot (AV) located on the experimental domain of Lavalette (IRSTEA Montpellier:
124 43.6466 °N ; 3.8715 °E) covers an area of 490 m², equipped with four rows of quasi-joined agrivoltaic
125 panels (PV) oriented North-South. The rectangular panels are 2 m long and 1 m wide for a total
126 surface coverage of 152 m². They are elevated at 5 m and part of a metallic structure supported by
127 pillars separated by 6.4 m, forming square arrays, so as to allow agricultural machinery in the
128 agrivoltaic plot. This coverage corresponds to a "half-density" in comparison with a classical free-
129 standing plant. The tilting angle of the PV may vary between -50° and +50° with reference to the flat,
130 horizontal case. This 1-degree of freedom rotation around the horizontal, transverse axis of the
131 panels is ensured by jacks. These may be controlled for solar tracking during daytime or to obey
132 other user-defined time-variable controls. The measurement campaign spreads from October 18th,
133 2015 to October 24th, 2016 thus covers a full year. It encompasses 41 monitored rain events, 12 of
134 which recorded with a 1-minute time step, among which 11 exhibit complete and reliable sets of
135 data linked to the incoming and redistributed rain amount, and to the tilting angle of the panels.

Supprimé: engines

136

137 **2.1.2. Effective rain and soil water content measurements**

138 The monitoring of rain amounts in the AV plot is ensured by a series of 21 collectors of 0.3 m
139 diameter, aligned and joined so as to form a continuous line, centered under a PV row, and
140 transverse to it (Fig. 1). In the following, the collectors are termed P01 to P21 from West to East. In
141 addition P0 indicates the rain amount collected in control conditions, just beside the AV plot. All rain
142 amounts collected are expressed as water depths (with 1 mm = 1 L m⁻²). The recordings were made
143 for various angular positions of the PV, either held flat or inclined ($\pm 50^\circ$) or during time-variable
144 "avoidance strategies" that mainly consist in minimizing rain interception by the panels by deciding
145 their titling angle from wind direction. Rain amounts in the nearby control zone are measured with a
146 tipping bucket rain gauge (Young 52203, Campbell Sci.). A windvane anemometer (Young 05103-L,
147 Campbell Sci.) allows recording wind direction and velocity.

Supprimé: in abutment

148

151 [Fig.1 about here]



152

153

154 **Figure 1 - Effective rain and soil water content measurement under solar panels. Red arrows indicate the position of**
155 **neutron probes, on a line parallel to that of the collectors, 1 m before it. Some of the P01 to P21 collectors have been**
156 **identified on the picture for clarity.**

157

158 Soil water content is measured with neutron probes (probe 503DR Hydroprobe, CPN International)
159 until 1 m depth. The soil is predominantly silty and deep. Seven neutron probes were installed at 0.0,
160 0.5, 1.0 and 3.2 m on both sides of the axis of rotation of the PV row (Fig. 1). Measurements are
161 made once or twice a week on a regular basis but systematically before and after the events.

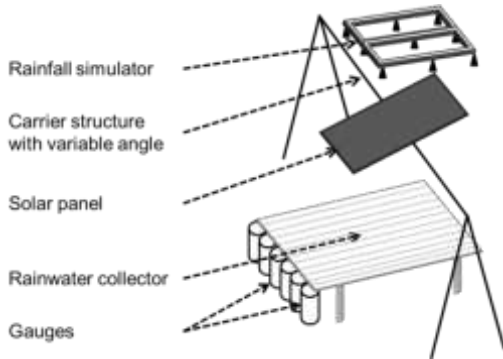
162

163 **2.1.3. Experiments in controlled conditions**

164 A reduced-size agrivoltaic device was built to characterize the influence of the tilting angle of the
165 panels in indoor conditions, monitoring the collected rain amounts in absence of wind with a focus
166 on the lateral redistribution on the width of the panels (Fig. 2). The experimental device consisted of
167 a (2 m x 1 m) panel on a supporting structure of reduced height, allowing tilting angles between 0
168 and 70°. A rainfall simulator composed of numerous fogging sprays was placed 1.8 m above the flat
169 position of the panel, ensuring quasi-uniform rain conditions on the whole area of the panel, with
170 tested intensities of 20, 35, 60 and 70 mm h⁻¹ selected to be representative of the local rain
171 intensities (corresponding to 1, 3, 16 and 32 years return periods, respectively). Water flowing out of
172 the panel was collected on a tilted plane on which 10 half cylinders were fixed, pouring water in the
173 corresponding 10 joined collectors of 0.1 m diameter, covering the width of the panel. The collected
174 amounts were weighted at the end of each test and converted into water depths.

175

176 [Fig. 2 about here]



177

178 **Figure 2 - Experimental device used for indoor tests, focusing on lateral rain redistribution on the width of the panel, for**
179 **various combinations of rain intensities and tilting angles of the panel.**

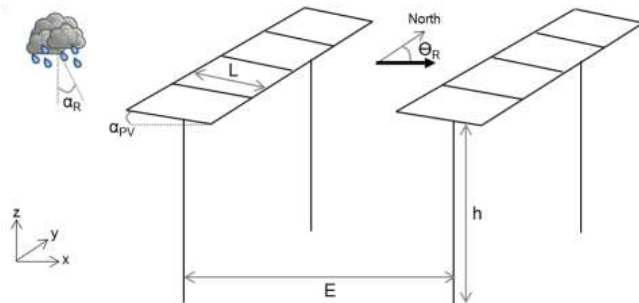
180

181 *2.3. Rain redistribution model (AVrain)*

182 **2.3.1. Model rationale**

183 The modelling of rain redistribution by solar panels is a geometrical problem describing rain
184 interception by an impervious surface of length L , tilting angle α_{PV} and height h above the ground, in
185 which α_R is the angle of incidence of rainfall with respect to the vertical axis and θ_R denotes the plane
186 in which the rain falls, with respect to the North in the present case (Fig. 3). The solution is studied in
187 the vertical (x, z) plane so that the effects in the y direction will be discussed and evaluated but not
188 explicitly described here. Finally, E is the spacing between the supporting pillars, allowing the
189 estimation of an equivalent 1-D surface coverage thus the extension of local calculations to the
190 whole agrivoltaic plot.

191 [Fig. 3 about here]



192

193

Supprimé: All notations appear in the Appendix.

Supprimé: ¶

¶
¶
¶
¶
¶
¶

204 Figure 3 - Scheme of the simulated scene, indicating the key parameters of the AVrain model that describes rain
205 redistribution by the solar panels on agrivoltaic plots.

206
207 The angle of incidence (α_R in degree) of rainfall with respect to z may be estimated from the ratio
208 between wind velocity (v_w in $m s^{-1}$) and the velocity of the falling rain drops (v_d in $m s^{-1}$), according to
209 Van Hamme (1992).

$$\tan(\alpha_R) = \frac{v_w}{v_d} \quad (1)$$

210 In the above, v_d is drawn from the equation proposed by Gunn and Kinzer (1949) for the free-fall limit
211 velocity of a rain drop in stagnant air, from measurements obtained with the electrical method,
212 relevant for drop diameters between 0.1 and 5.7 mm:

$$v_d^2 = \frac{4 g D (\rho_s - \rho)}{3 \rho c} \quad (2)$$

213 where g is the acceleration of gravity ($m s^{-2}$), ρ_s is water density ($kg m^{-3}$), ρ is air density
214 ($kg m^{-3}$), D is the drop diameter (m) and c is the drag coefficient (-).

215 Drop size distribution has been linked to rain intensity (I in $mm h^{-1}$) by Best (1950) from previous
216 literature elements and measurements made by the author:

$$1 - F_{cum} = \exp\left(-\left(\frac{D/1000}{1.3 I^{0.232}}\right)^{2.25}\right) \quad (3)$$

217 where F_{cum} is the fraction of liquid water in the air comprised in drops with diameters less than D.
218 The determination of the angle of incidence of rainfall (α_R , °), from given rain intensity (I) and wind
219 velocity (v_w) allows then
220 - to discriminate the zones impacted by the presence of solar panels from these that will receive the
221 same rain amounts as in the control zone,
222 - to calculate the water amount intercepted by the solar panels (I_{PV} , mm^{-1}) in function of I, α_{PV} (°), α_R
223 (°), θ_{PV} (°N) and θ_R (°N), after Van Hamme (1992):

$$I_{PV} = I (\cos \alpha_{PV} - \tan \alpha_R \sin \alpha_{PV} \cos(\theta_{PV} - \theta_R)) \quad (4)$$

224 For simplicity, it is assumed that no significant lateral redistribution occurs on the width of the
225 panels, resulting in no variation of the outlet flow in the transverse y direction. The relevance of this
226 hypothesis is justified in the following: the tests in indoor conditions were designed to address this

Supprimé: (D)

Supprimé:

Supprimé: c

Supprimé: c

231 issue. It is also assumed that the wetting phase of the panels before runoff initiation (somehow the
 232 storage capacity of the panels) has no noticeable effects on the calculations. From observations, for
 233 low tilting angles, the I_{PV} value needed to trigger runoff is 0.2 mm at most which is a small value
 234 compared to the other values involved in the analysis (and lower than the usual precision of rain
 235 gauges).

Supprimé: weak

236 Runoff velocity (V , $m s^{-1}$) is calculated with the Manning-Strickler formula, hypothesizing flow width is
 237 much larger than flow depth, which makes flow depth approximately equal to the hydraulic radius.
 238 Manning's n coefficient is assumed to be $0.01 s m^{-1/3}$ after (Chow, 1959) because of the very smooth
 239 glass coating of solar panels.

Supprimé: ^{1/3}

Supprimé: Te

240 The parabolic trajectory of the drops falling from the panels is calculated in similar ways for any drop
 241 size (i.e., diameter D) and characterized by the abscissa at which the free falling drop touches ground
 242 (x^* , m) and the free fall duration (t^* , s):

$$\begin{cases} x^* = a_x \frac{t^{*2}}{2} + V \cos \alpha_{PV} t^* + x_0 \\ a_x = 2 \cdot 10^{-4} \frac{v_w^2}{D/2} \\ t^* = \frac{V \sin \alpha_{PV} + \sqrt{(V \sin \alpha_{PV})^2 + 2 g z_0}}{g} \end{cases} \quad (5)$$

243 where a_x is the acceleration ($m s^{-2}$) due to wind in the x direction, considering a drag coefficient of
 244 $c=0.5$ for the drops in the air, V is the initial velocity of the fall ($m s^{-1}$) and x_0 is the abscissa of the
 245 edge of the PV (m).

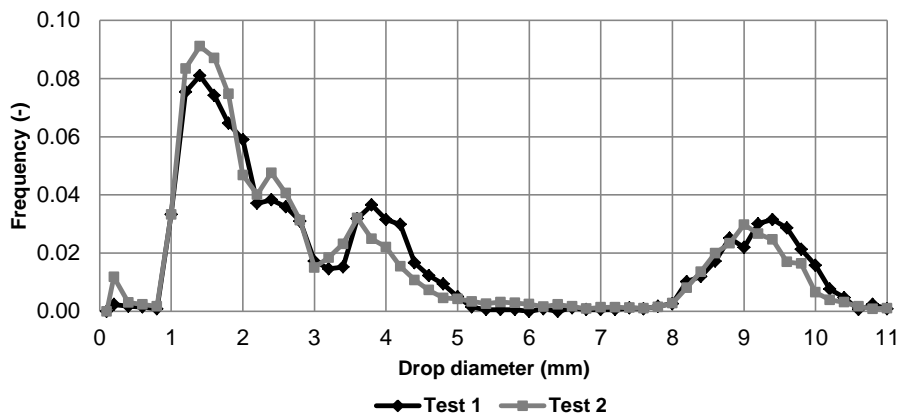
Supprimé:

246 Drop diameter measurements (expressed further in mm for convenience) were conducted with a
 247 dual-beam spectropuviometer (Delahaye et al., 2006). A three-mode distribution of drop diameters
 248 was revealed with peaks at $D=1.4$, 3.8 and 9.3 mm (Fig. 4). However, diameters $D > 7.5$ mm (Niu et
 249 al., 2010) might be artifacts because rain drops this size would become unstable and split in two
 250 droplets during their fall. In the following numerical applications, a fixed diameter of $D=1.5$ mm is
 251 selected as the reference case for simplicity. However, the sensitivity of the model to D is low and
 252 will be discussed later.

Supprimé: and revealed a

Supprimé: weak

253
 254 [Fig. 4 about here]



261

262

263 Figure 4 - Drop-size distribution curve, obtained with a dual-beam spectrop pluviometer, for the drops falling from the
 264 edge of the solar panels. The frequency plotted on the y-axis indicates the count of diameters D observed with respect to
 265 the total count (the step is about 0.2 mm for D).

Supprimé: Granulometric

266

Supprimé: in

267 The AVrain model was developed with the R software to describe 2D (x, z) phenomena in the vertical
 268 plane, hypothesizing negligible effects in the transverse (y) direction (Fig. 1). The time step of AVrain
 269 is 1 minute. The required climatic forcings are: rain intensity (I), wind velocity (v_w) and direction (θ_R)
 270 which is assumed identical to rain direction. The input parameters are the geometrical descriptors of
 271 the structure: the height of (the axis of rotation) of the panel (h), its length (L), tilting angle (α_{pv}) and
 272 orientation (θ_{pv}), plus the spacing between (pillars supporting the) solar panels (E). Only the tilting
 273 angle can be a function of time as it denotes the control exerted on the system. AV rain allows
 274 calculating rain redistribution (in x) in the form of effective cumulative rainfall amounts in function of
 275 time. A known limitation of this simplified model is that the effects of the secondary slopes of the
 276 panels are not explicitly accounted for, although properly identified by the experiments in controlled
 277 conditions. These have shown that the combination of low tilting angles (i.e. primary slopes $\alpha_{pv} < 5^\circ$)
 278 and low rain intensities lead to lateral dispersion on the edge of the panels. In these cases, this leads
 279 to concentrate water fluxes on the lower corner of the panel. However, the impact on the water
 280 balance (and its heterogeneity) is limited due to the low magnitude of the corresponding rainfall
 281 amounts, as discussed in section 4.1.

Supprimé: homogeneities

Supprimé: ,

Supprimé: at the risk of concentrating

Supprimé: in extreme cases

Supprimé: the magnitude of this rain redistribution remains limited in the present experimental and is

282

Supprimé: the following

293 **2.3.2. Sensitivity analysis**

294 The implementation of solar panels is very likely to affect crop management and irrigation strategies
295 in the equipped plots, especially because of rain redistribution by the panels. The associated patterns
296 of spatial heterogeneity may be described by the coefficient of variation (Cv) closely related to the
297 coefficient that describes the uniformity of water distribution by the irrigation systems (ASAE, 1996;
298 Burt et al., 1997), thus allowing easy comparisons. The choice of Cv as the target variable for
299 sensitivity analysis acknowledges spatial heterogeneity is the key descriptor of the effects of solar
300 panels on rain redistribution on the cultivated plots. In the following, Cv is calculated from the
301 effective rain amounts (i.e., the cumulative water depths) simulated in the 21 joined collectors along
302 the x axis. High Cv values indicate strong heterogeneities while values below 0.2 will be considered as
303 acceptable, according to the standards of ASAE (1996) for irrigation uniformity. This threshold of 0.2
304 is also consistent with the reference values reported in Van der Gulik et al. (2014).

Supprimé: and Table

Supprimé: 1, adapted from

Supprimé: , recalls the range of Cv values used to qualify the uniformity of water distribution by the irrigation systems

Supprimé: Burt et al. (1997)

Supprimé: ¶
¶
¶
¶
¶
¶
Table 1 - Reference values for the coefficient of uniformity of water distribution by irrigation systems, after ASAE (1996) and Burt et al. (1997). The original values are expressed here as values of the coefficient of variation used to measure the spatial heterogeneity of rain redistribution by the solar panels.¶
¶
Performance

306
307
308 Using Cv as an indicator allows accounting for two sources of spatial heterogeneity: rain
309 redistribution by the solar panels (with eventual local effective rain amounts that exceed the
310 "natural" rain amounts measured in the control zone) and the sheltering effect of solar panels (with
311 effective rain amounts far lower right under the panels than in the control zone). More into details,
312 Cv encompasses in a single indicator the spatial heterogeneity observed within the region located
313 right under a solar panel, i.e. centered on the transverse y axis that connects two supporting pillars,
314 as clearly seen in Fig. 1 where the P11 is the central collector. The width of the equipped region is E,
315 selected as the parameter that describes the spacing between panels and further used to estimate
316 the 1-D spatial coverage of the plot by the panels, also taking place in the sensitivity analysis of the
317 model.

318
319 The Morris (1991) method is used with Cv as the target variable, to estimate the sensitivity of the
320 AVrain model to assess the effect of its seven main parameters (see Table 2) on the spatial
321 heterogeneity of rain redistribution by the solar panels. The combined "one-at-a-time" screenings of
322 the parameter space introduced by Campolongo et al. (2007) have been used to cover a wide set of

346 possible agrivoltaic installations, keeping all parameters within acceptable, realistic ranges of values.
 347 The "sensitivity" package of R (Pujol et al., 2017) was used to generate the associated 4000
 348 parameter sets, obtained from $p=7$ parameters with $d=500$ draws each, dispatched within $r=8$ levels.
 349 The control parameter (tilting angle θ_{PV} of the panels) was taken between -70° and $+70^\circ$ but held
 350 fixed for the tested event ($P=3.6$ mm, $v_w=0.78$ m s^{-1} , $\theta_w=285^\circ$, described later).

351

352 **Table 1-** Parameters and ranges of values used in the sensitivity analysis of the AVrain model

Supprimé: 2

Parameter	Description	Reference	Range	Unit
D	Size of the drops falling from the solar panels	1.5	0.1 - 7	mm
E	Spacing between solar panels	6.40	4 - 10	m
FactorP	Multiplying factor for precipitations	1	0.1 - 10	-
FactorV	Multiplying factor for wind velocity	1	0.1 - 10	-
H	Height of the solar panels	5.00	3 - 7	m
L	Lenght of the solar panels	2.00	1 - 3	m
θ_{PV}	Tilting angle of the solar panels	0	-70 - 70	°

353

354

355 2.4. Control simulations of soil moisture field by Hydrus-2D

356 Hydrus-2D (Simunek et al., 1999) may be used to simulate water redistribution in soils for different
 357 fixed tilting angles of the solar panel or strategies in operating the panels. The simulation domain
 358 finds itself in a vertical (x, z) plane, it is centered on the supporting pillar of a panel and covers a total
 359 width of 6.4 m, corresponding to the distance between two consecutive pillars. Hydrus-2D is rather
 360 used here for coherence checks and to gain an overview of water redistribution in soil than for
 361 detailed numerical simulations of the wetting front movements in space and time, thus allowing
 362 simplifying hypotheses on soil structure. The investigated soil depth is 1-m deep, well-known from
 363 numerous local experiments_s and predominantly silty. It is assumed homogeneous in absence of
 364 significant contrast with depth and presented in Table 3.

Supprimé: 1

365

366

369

370 **Table 2-** Soil parameters at the Lavalette experimental station used in Hydrus-2D, after Barakat et al. (2017, submitted).

Supprimé: 3

371 θ_r and θ_s denote respectively the residual and saturated volumetric soil water contents, α and n are empirical shape
372 parameters of Van Genuchten-Mualem model, K_s is the soil hydraulic conductivity at saturation and l is a pore
373 connectivity parameter.

374

Depth (cm)	Clay (%)	Silt (%)	Sand (%)	θ_r (cm ³ /cm ³)	θ_s (cm ³ /cm ³)	α (cm ⁻¹)	n (-)	K_s (cm hr ⁻¹)	l (-)
0 – 100	18	42	40	0.01	0.36	0.013	1.2	2.30	0.5

Supprimé: (-)

Supprimé: -

375

376 The AVrain model provides the time-variable forcing data at the soil-atmosphere interface for
377 Hydrus-2D, divided into five categories and accounting for time-variable tilting angles of the solar
378 panel (Fig. 5):

Supprimé: ¶

- 379 - atmospheric conditions for zones not impacted by the presence of the solar panel,
- 380 - flux 1 (F1) conditions for zones impacted by the panel and located right under it,
- 381 - flux 2 (F2) conditions for zones impacted by the panel but not located under it,
- 382 - flux 3 (F3) conditions for zones located under the edge of the panel thus exposed to the largest
383 effective rain amounts,
- 384 - flux 4 (F4) conditions for zones adjacent to these of the F3 conditions but on the sheltered side.

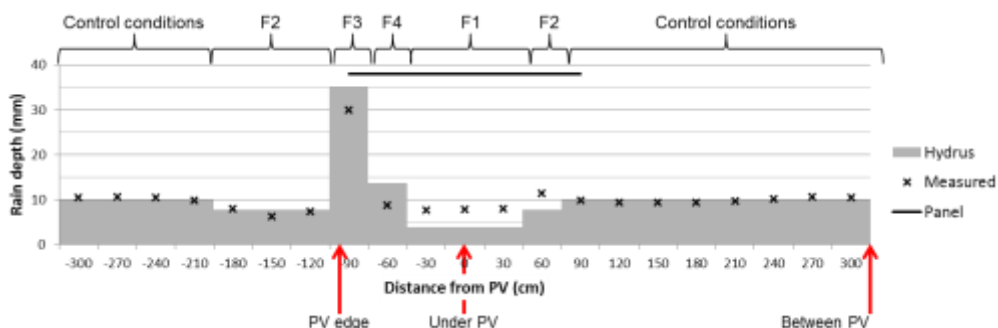
385

386 Hydrus-2D currently allows five types of time-variable upper boundary conditions, which suggests
387 using F2 on both sides of the panel, as indicated in Fig. 5 where only the leftmost position of F2
388 corresponds to the choices listed above. However, the rightmost position of F2 seems the most
389 suitable default choice given the known soil filling dynamics and the expected effective rain amounts.
390 Zero-flux boundary conditions apply on the vertical limits of the domain and free drainage is relevant
391 for a bottom boundary condition because the water table is several meters under the limit of the
392 domain. For simplicity, the initial soil water content will be assumed homogeneous, selecting a value
393 close to the available observations ($\theta=0.15$).

394

395

400 [Figure 5 about here]



401
402 **Figure 5 - Time-variable upper boundary conditions used in Hydrus-2D for the tested rain event, during which the tilting**
403 **angle of the panels was varied to minimize rain interception (avoidance strategy).**

404
405 **3. Results**

406 *3.1. Rain redistribution measurements on the dynamic agrivoltaic plot*

407
408 The influence of variable-tilting angle solar panels on rain redistribution was measured ~~thanks to a~~
409 wide series of rain events covering a full year. ~~For each event, we put a focus on the spatial~~
410 ~~heterogeneity, which is assumed to be a crucial issue for the hydrological balance of solar panels on~~
411 ~~crops. This heterogeneity is characterized with the coefficient of variation Cv of rain depths.~~ Table 4
412 gathers Cv values obtained for the most documented rain events in the available records. It enables
413 comparisons between Cv and the tilting angle (or operating strategy) of the solar panels, for various
414 rain intensities. The least heterogeneous rain redistributions were observed for panels in abutment
415 (Fig. 6a, b) mainly due to decreased surface coverage, from 30% for flat panels to 20% for panels in
416 abutment, resulting in a lesser rain interception. However, the relevancy of this strategy depends on
417 the angle of the wind with respect to the panels (α_R vs. θ_R) identifying these as second-order but non-
418 negligible factors, according to which Cv may become twice as large for panels "facing the wind" or
419 "back to the wind". By contrast, the most heterogeneous rain redistribution was observed for a flat
420 panel ($\alpha_{PV}=0$) maximizing rain interception and concentration by the panel (Fig. 6c), collecting 11
421 times more rain than in the control zone, in the F4 domain of Fig. 5, with $Cv=2.13$.

Supprimé: for
Supprimé: ,
Supprimé: taking
Supprimé: coefficient of variation (Cv) as the target variable thus assuming this measure of spatial heterogeneity is the crucial hydrological descriptor in agrivoltaic contexts

431 Strategies involving time-variable tilting angles α_{pv} offer multiple possibilities, among which the
 432 previously mentioned "avoidance strategy" is relevant to decrease the spatial heterogeneity (Fig. 6d)
 433 and results in $Cv=0.22$, that is a fairly good homogeneity according to Table 1. For all the events listed
 434 in Table 4, only the avoidance strategy was able to provide an acceptable level of uniformity in the
 435 agrivoltaic plot, i.e. a spatial heterogeneity than would not need to be corrected on purpose, with a
 436 dedicated precision irrigation device, to ensure equivalent water availability conditions during crop
 437 growth. In all cases, the effective rain depth was more important on the sides of the panel (collectors
 438 9 and 13 in Fig. 1 and Fig. 6). There are non-impacted zones in the free space between panels, where
 439 the effective rain is the same as in the control zone. On the contrary, the sheltering effect is strong
 440 right under the panels and the effective rain is always far lower than in natural conditions.

441

442 **Table 3-** Rain events with their identification (ID), date, rain amounts on the control zone (P0), tilting angle of the solar
 443 panels (α_{pv}) and the associated measured coefficient of variation (Cv) whose highest values indicate the strongest spatial
 444 heterogeneities in rain redistribution by the solar panels. In the comments Sect., "avoidance strategy" indicates a time-
 445 variable α_{pv} angle to minimize rain interception by the panels in real time.

Supprimé: 4

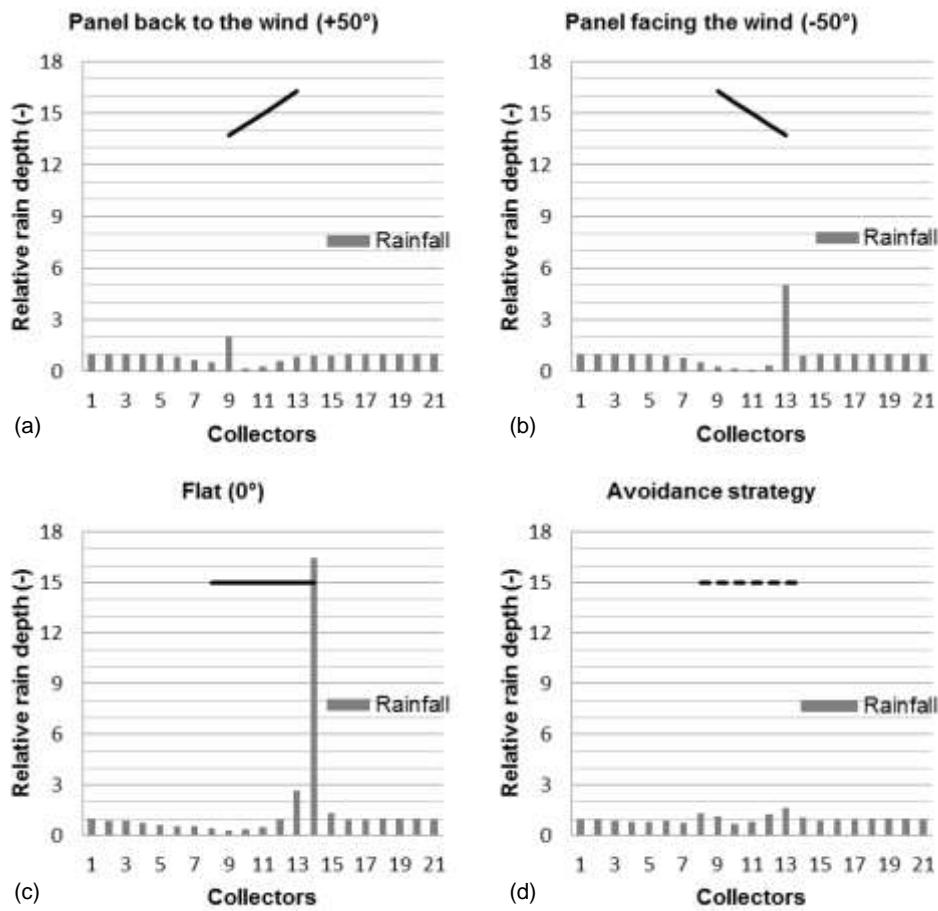
446

ID	Date	P0 (mm)	α_{pv}	Cv (-)	Comments
#01	18/10/2015	4.8	-50 to 0°	1.14	Solar tracking
#02	07/12/2015	5.1	-50 to -30°	0.98	Solar tracking
#03	12/02/2016	14.6	-50°	0.97	Transverse wind (south)
#04	09/03/2016	5.1	-50°	0.96	Facing the wind
#05	17/03/2016	4.1	+50°	0.40	Back to the wind
#06	21/04/2016	3.6	0°	2.13	Flat panel
#07	30/04/2016	3.0	0°	1.15	Flat panel
#08	22/05/2016	8.4	0°	0.72	Flat panel
#09	28/05/2016	13.5	0°	1.28	Flat panel
#10	31/05/2016	4.5	0°	1.63	Flat panel
#11	14/09/2016	14.8	-50 to +50°	0.22	Avoidance strategy
#12	12/10/2016	203.6	0°	0.51	Flat panel

447

448 [Figure 6 about here]

Supprimé: 1



451
 452 **Figure 6 - Examples of rain redistribution for various rain events, tilting angle and operating strategies of the solar panels,**
 453 **measured in the collectors displayed in Fig. 1. Relative rain depths are given with respect to the control zone where rain**
 454 **amounts are collected in the pluviometer.**

455
 456 *3.2. Evaluation and sensitivity analysis of the AVrain model*

457
 458 The rain redistribution model AVrain was tested for 11 rain events involving flat panels, panels in
 459 abutment (either back to the wind or facing the wind) and avoidance strategies, as presented in
 460 Table 5. AVrain describes rain redistribution with a satisfying mean determination coefficient of
 461 $R^2=0.88$. The values of MAPE (Mean Absolute Prediction Error) mostly comprised between 0.1 and
 462 0.3 and regression coefficients greater than 1 indicate that the model tends to overestimate the real

463 effective rain amounts. However, Fig. 7 shows that the overestimations occur near the drip line (i.e.,
 464 the aplomb) of the panels, totaling about 25% of the committed errors.

465

466 **Table 4-** Performances of the AVrain model that describes rain redistribution by the solar panels, identifying each event
 467 (ID), indicating the Mean Absolute Prediction Error (MAPE), Normalized Root Mean Square Error (NRMSE), linear
 468 correlation coefficient and coefficient of determination (R^2) next to the simulated coefficients of variation (Cv). The
 469 highest Cv values signal the strongest spatial heterogeneities in rain redistribution by the solar panels.

Supprimé: 5

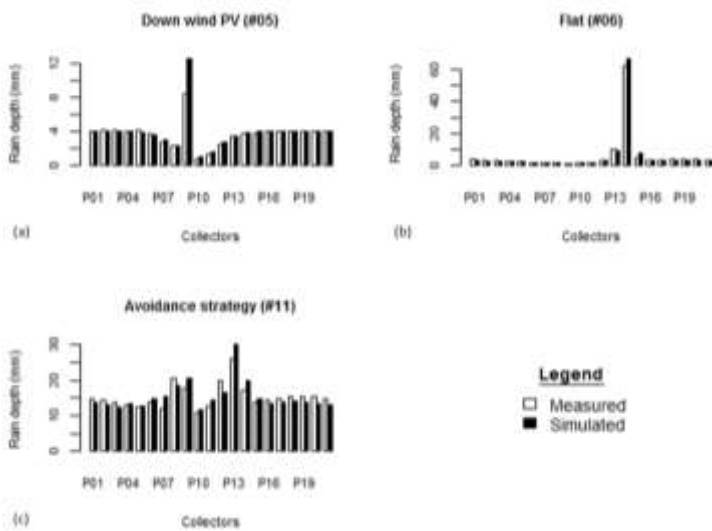
470

ID	MAPE	NRMSE	<u>Slope of regression</u> <u>line</u>	R^2	Cv
#01	0.29	0.22	1.21	0.89	1.15
#02	0.25	0.22	1.45	0.86	1.21
#03	0.41	0.10	0.82	0.83	0.75
#05	0.07	0.13	1.10	0.86	0.46
#06	0.14	0.13	1.06	1.00	2.28
#07	0.21	0.20	0.89	0.98	1.25
#08	0.13	0.11	0.88	0.99	0.72
#09	0.23	0.12	1.38	0.97	1.50
#10	0.22	0.17	1.04	0.96	2.34
#11	0.11	0.08	1.00	0.75	0.19
#12	0.17	0.03	1.13	0.56	0.78

Supprimé: Linear correlation coefficient

471

472 [Figure 7 about here]

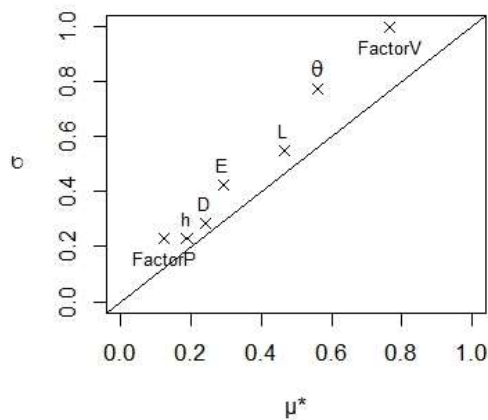


475
 476 **Figure 7 - Examples of rain redistribution by the solar panels simulated by the AVrain model and compared to field**
 477 **measurements, for three very different events and managements of the solar panels (see Tables 4 and 5 for details).**

478
 479 The sensitivity analysis of AVrain was conducted with the Morris (1991) method, modified and
 480 improved by Campolung et al. (2007), selecting C_v as the target variable. Figure 8 shows its results,
 481 where μ^* on the x-axis is the mean of the individual elementary effects (thus the sensitivity of the
 482 parameter tested alone) and σ on the y-axis represents the standard deviation of the elementary
 483 effects (thus the sensitivity of the parameter tested in interaction with other parameters). The Morris
 484 plot allows identifying the parameters that have i) a negligible overall effect, denoted by low values
 485 of both μ^* and σ , ii) a linear effect, denoted by high values of μ^* , or iii) non-linear or interactive
 486 effects, denoted by high values of σ . The sensitivity measures (μ^* , σ) reported in Fig. 8 for each
 487 parameters have been normalized by the value of the highest sensitivity measure (σ) for the most
 488 sensitive parameter (FV).

489
 490 [Figure 8 about here]

Supprimé: ¶
 ¶
 ¶
 ¶



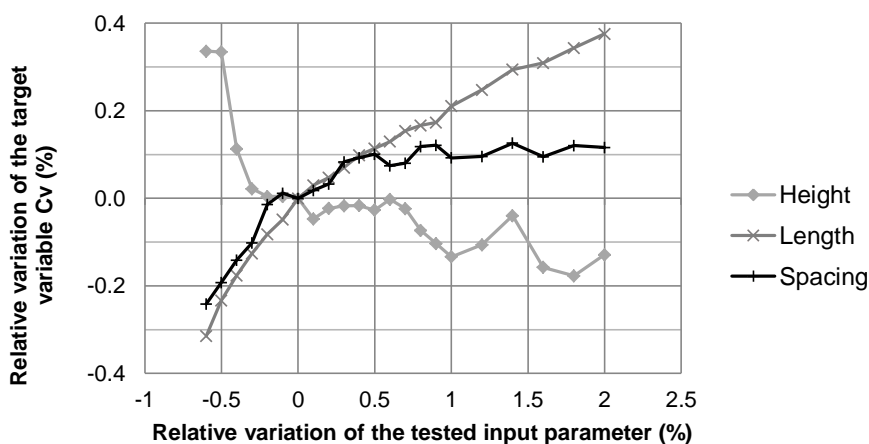
495
 496 **Figure 8 - Sensitivity analysis of the AVrain model by the Morris (1991) method improved by Campolongo et al. (2007),**
 497 **where μ^* indicates the linear part of the total sensitivity score for each parameter while σ indicates the non-linear or**
 498 **interactive part. In the Morris plot, D is the drop diameter, E the spacing between solar panels, FP the multiplying factor**
 499 **for precipitations with respect to the reference case, FV the multiplying factor for wind velocity with respect to the**
 500 **reference case, h the height of the solar panels, L their length and θ_{pv} their tilting angle (see Table 2 for the reference**
 501 **values and ranges of the parameters). The target variable of the analysis was the coefficient of variation that measures**
 502 **the spatial heterogeneity of rain redistribution by the solar panels. The tested rain event was #06 in Tables 4 and 5.**

503
 504 Supprimé: ¶ The position of the parameters above the 1:1 line in Fig. 8 signals that AVrain is more sensitive to the
 505 interactions between parameters than to individual variations of the parameter values which
 506 reinforces the fact that strong heterogeneities in effective rain amounts most likely occur when
 507 several conditions are met at once, in the forcings (wind direction, drop size), the controls (tilting
 508 angle) and the structure (fixed characteristics of the panels). In particular, the high sensitivity score of
 509 FV compared to the low score of FP indicates that wind velocity tends to influence rain redistribution
 510 patterns far more than rain amounts, likely because wind velocity intervenes in the calculation of the
 511 angle of incidence of rainfall and in that of the trajectory of the drops falling from the panels. The
 512 drop size itself was found of non-negligible but of rather weak influence, although a wide range (0.1
 513 to 7.0 mm) of values was tested. The fact that AVrain is more sensitive to the tilting angle (control
 514 exerted on the system) than to the structure parameters (fixed once selected during the installation)
 515 is a crucial result of the analysis, indicating there is room for optimisation. Conversely, the higher

517 sensitivity of AVrain to wind velocity than to the tilting angle confirms that the optimisation
 518 strategies should be decided from wind characteristics that dictate the angle of incidence of rainfall.
 519 In an overview of Fig. 8, the Morris method unveils the hierarchy of effects. This proves especially
 520 useful when investigating the interactions between the structure parameters. For example, the
 521 combinations between panel length and spacing (defining surface coverage) are expected to have
 522 more effect on the target variable than the combinations involving panel height, making height a
 523 second-order parameter, at least for the tested (realistic) ranges of values and the chosen target
 524 variable. This conclusion would have been impossible to reach when separately testing the effects of
 525 variations in length, spacing and height of the panels, as proven by Fig. 9 which only acknowledges
 526 adverse effects (on Cv) of length and spacing on the one side, and of height on the other side.

Supprimé: s

527
 528 [Figure 9 about here]



529
 530 Figure 9 - Spider diagram showing the influence of the structure parameters (spacing E, height h, length L) of the
 531 agrivoltaic installation on the spatial heterogeneity of rain redistribution by the solar panels, from the simulated values
 532 of the coefficient of variation (Cv).

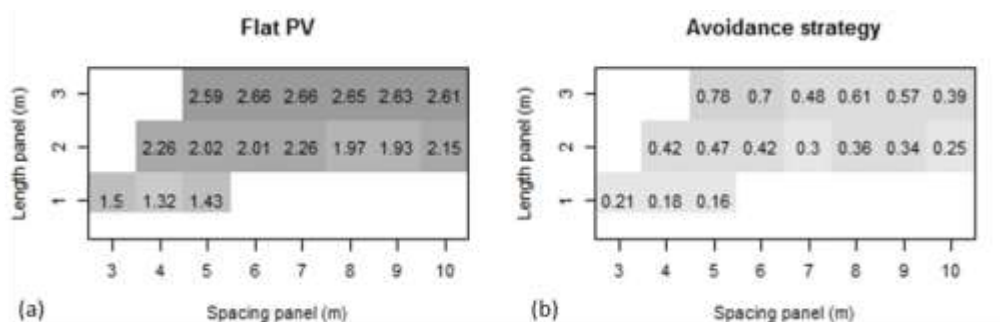
533
 534 From Fig. 8, the influence of the tilting angle may be expected larger than that of the structure
 535 parameters, anticipating thus that the avoidance strategy (i.e., operating the panels so as to
 536 minimize rain interception) will be prone to significantly reduce Cv whatever the structure
 537 parameters. This point is further investigated by Fig. 10, comparing a flat panel with a piloting of the

539 panel according to the avoidance strategy, for various combinations of panels length and spacing
 540 (previously proven to have more influence on Cv than the height of the panels). Small-sized panels
 541 with a low spacing between them is advocated as the best configuration to reduce Cv in avoidance
 542 strategies, simulated to be far more efficient than panel held flat. However, this analysis indicates the
 543 direction to follow when only rain redistribution issues are tackled but external constraints will surely
 544 exist when deciding the in-situ implementation of such agrivoltaic installations, for example in the
 545 form of limit values for the spacing between panels (to allow agricultural activities).

Supprimé: weak

546

547 [Figure 10 about here]



548

549 **Figure 10 - Influence of the structure parameters (spacing E, length L) of the panels on the spatial heterogeneity of rain**
 550 **redistribution, from the simulated values of the coefficient of variation (Cv) for panels held flat (a) or operated according**
 551 **to the avoidance strategy (b). The combinations of E and L values may be assimilated to equivalent 1-D surface coverage**
 552 **between 20 and 60% by dividing L by E. Only the realistic combinations have been simulated here: blank cells indicate**
 553 **those that are not.**

554

555 3.3. Rain redistribution in soils

556

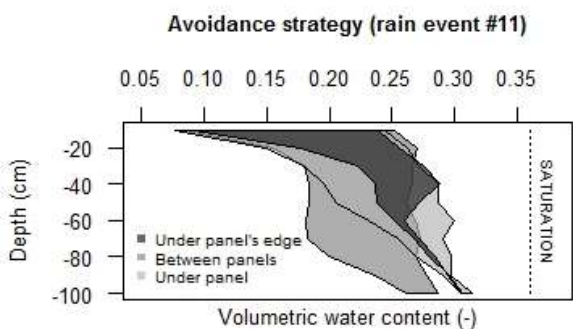
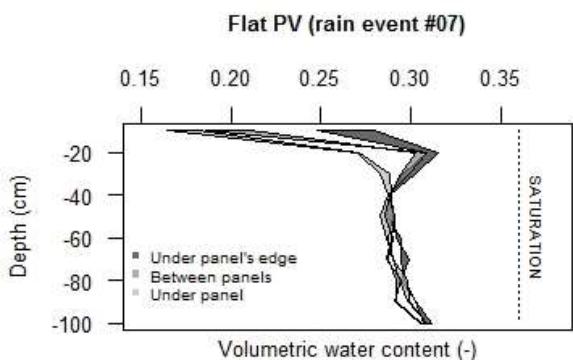
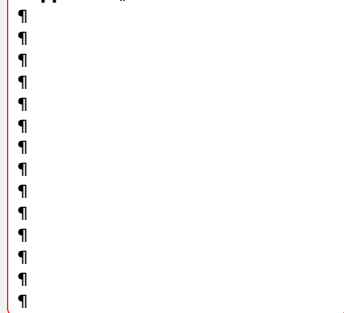
557 Water content profiles were measured in the agrivoltaic plot immediately before one of the rain
 558 events, then 6 to 12 hours after it, to identify the dynamics and magnitude of rain redistribution in
 559 soils, as a consequence of rain redistribution on the soil surface. As expected, the spatial
 560 heterogeneity observed on the soil surface is transferred but becomes a bit fuzzy in the first 30 cm of
 561 soil, due to "lateral homogenization" (ponding with significant surface runoff, lateral diffusion
 562 associated with soil dispersivity). But still the spatial patterns are clearly visible within soils, especially

564 for the flat panels case (Fig. 11a) for which three distinct zones may be identified, i) between panels,
 565 with similar behavior as in the control zone, ii) under panels, with a noticeable sheltering effect thus
 566 drier soils and iii) under the edge of the panels, where the increased soil water content is attributable
 567 to the large effective amounts poured on the soil surface. In Fig. 11a, the maximal soil water storage
 568 variation was observed under the edge of the panels, estimated at 6.7 mm in accordance with the
 569 location of the effective rain amount poured on the soil surface (24.0 mm). Between panels, the
 570 storage variation was 2.0 mm for 3.0 mm of effective rain. Under panels, the storage variation was
 571 4.7 mm for only 1.3 mm of effective rain, which reinforces the hypothesis of lateral redistribution,
 572 either within the soil or at its surface, from the nearby zones. In Fig. 11b, the avoidance strategy
 573 tested for a rain event of 60 mm in the control zone resulted in a maximal storage variation of 91 mm
 574 between panels due to a drier initial soil water content, 76 mm under panels and 43 mm near the
 575 aplomb of the edge of the panels, while significant ponding was observed.

Supprimé: The

576
 577 [Figure 11 about here]

Supprimé: ¶



578

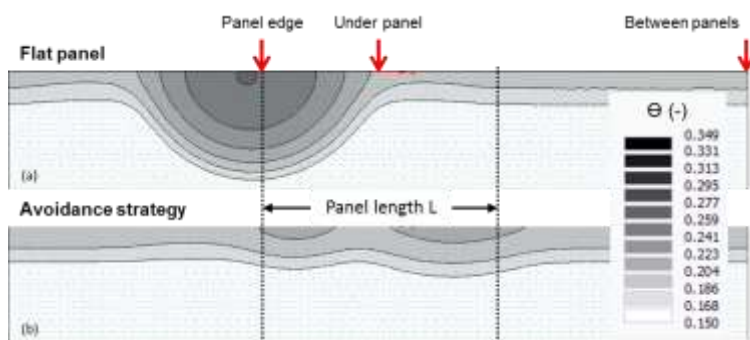
595 Figure 11 - Variations of soil water storage in soil regions located near the aplomb of panels edge (dark grey), between
596 panels (medium grey) and under panels (light grey) for different strategies in operating the panels, holding panels flat
597 during rain event #07 (a) or operating them according to the avoidance strategy that minimizes rain interception, during
598 rain event #11 (b). For each case, the leftmost and rightmost line indicates the water content profile before and after the
599 event, respectively. Event #11 was considered as the sum of two successive events for a total rainfall of 60 mm in the
600 control zone.

601

602 The simulation of rain redistribution in soils was made by Hydrus-2D for a single rain event (#11) to
603 compare the soil water content fields obtained in the flat panel case (Fig. 12a) or when using the
604 avoidance strategy (Fig. 12b). The time-variable atmospheric conditions required by Hydrus-2D were
605 provided by the outputs of AVrain at the minute time step, with the five-zone discretization
606 discussed in Sect. 2.4 and shown in Fig. 5. Starting from a rather dry, realistic and approximately
607 homogeneous soil water content of $\theta=0.15\text{cm}^3/\text{cm}^3$, the objective of these exploratory simulations
608 were not to capture the finest spatial patterns of the wetting front; it was rather to assess if the
609 observed noticeable differences in rain redistribution trends could easily be reproduced and
610 quantified by Hydrus-2D. As expected, the flat panel case leads to the creation of a sharp contrast of
611 soil water content, near the aplomb of the edge of the panel, in the form of a wet bulb that
612 propagates downward by gravity and sideward by diffusion. This result in the vertical plane is in
613 coherence with a well-known 3D effect of drip irrigation, that the vertical and horizontal
614 deformations of the ellipsoidal bulb will depend on soil properties: coarse soils will produce very
615 elongated bulbs in the vertical direction while silty soils are likely to produce more significant lateral
616 redistribution. However, the simulated spatial heterogeneities in soil water content remain very
617 pronounced for the flat panel case in comparison with the avoidance strategy (Fig. 12b). In this
618 manuscript, the choice of the coefficient of variation (Cv) to qualify the spatial heterogeneities
619 allowed the reconnection to the coefficient of uniformity classically used in irrigation science,
620 addressing water delivery on the soil surface, typically by sprinkler irrigation. Here, Fig. 12a
621 resembles the 2D or 3D patterns characteristic of surface or subsurface drip irrigation while Fig.12b
622 recalls the quasi-1D patterns of (high-performance) sprinkler irrigation.

623

624 [Figure 12 about here]



625
626
627 **Figure 12 - Simulation of soil water patterns with Hydrus-2D, in regions located near the aplomb of panels edge, under**
628 **panels or between panels, when holding the panels flat (a) or operating them according to the avoidance strategy (b) to**
629 **reduce the heterogeneity of rain redistribution by the panels, during Event #11 (see Tables 4 and 5). The vertical arrows**
630 **recall the positions of the neutron probes used to collect water content data plotted in Fig. 11.**

Supprimé: ¶

631
632 *3.4. Effects of the transverse slope of the panels*

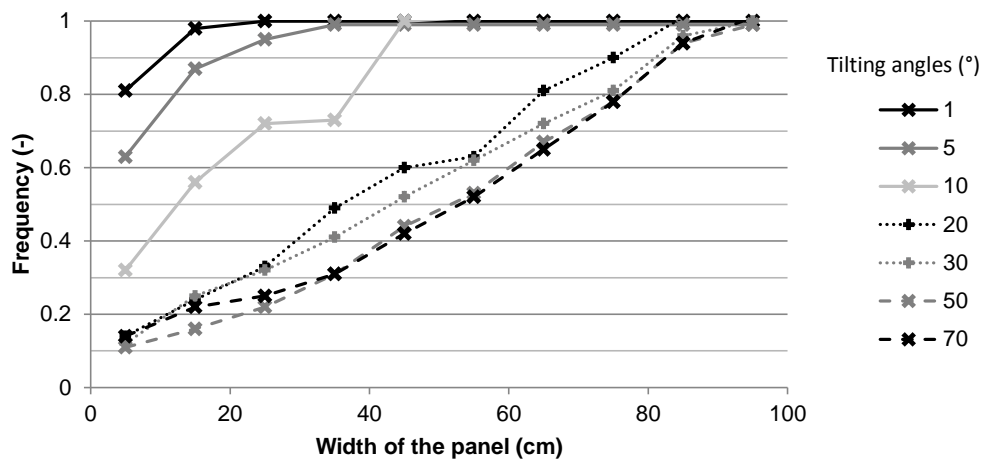
633
634 The underlying hypotheses made in the construction of the AVrain model led to the formulation of a
635 2D (x, z) model, discarding thus all phenomena arising from variations in the transverse (y) direction
636 or, at least, not representing them in explicit manner. If relevant, indirect assessments of their effects
637 should still be made, outside AVrain but to investigate if the model stays valid -or in which conditions
638 significant uncertainties may exist on its predictions. Among transverse effects likely to exist in real
639 conditions, only the effects of transverse slopes of the panels were anticipated, observed and
640 deemed significant, though limited to particular contexts. These contexts are summed up in the cases
641 when the tilting angle (i.e. the prevalent slope) of the panels is very low, so that the transverse,
642 secondary slope becomes of the same order.

643
644 Tests in controlled conditions were conducted during 15 minutes, under a rain intensity of 20 mm h⁻¹.
645 Rain redistribution on the width of the panel appears for tilting angles lower than 20° and the width
646 of the outlet becomes very narrow for tilting angles lower than 5° (Fig. 13). In the latter case, about
647 90% of the collected water drops from the panel through a 20-cm wide outlet. In the general case,
648 such effects may be explicitly calculated from the slopes (prevalent, secondary) and water depth on

650 the panel. Such effects are prone to increase the effective rain amounts observed in the field, at the
651 aplomb of the edge of the flat panels (Fig. 6c).

652

653 [Figure 13 about here]



654

655 **Figure 13 - Influence of the transverse slope of the solar panels on the lateral rain redistribution on the width of the**
656 **panel, tested for a 20 mm h⁻¹ rain intensity and "prevalent" tilting angles of the panels between 1 and 70°. The results**
657 **are expressed in cumulative distribution of the collected amounts, at the outlets placed along the width of the panel.**

658

659 4. Discussion

660 4.1. Rain redistribution by the solar panels

661

662 The 2D AVrain model was developed to describe rain interception and redistribution by the solar
663 panels and fulfills its objectives well: it allows the identification of the sheltered zones and of the
664 zones in which the effective rain amounts exceed the natural rain amounts of the control zone, with
665 a correct quantification of the associated fluxes. The angle of incidence of rainfall was found a key
666 variable in the determination of the spatial patterns of heterogeneity in the effective rain amounts
667 falling on the ground. This angle is difficult to measure but the equations derived by Gunn and Kinzer
668 (1949) and Best (1950) allow to estimate it in indirect ways.

669

670 If relevant, the AVrain model may be adapted to account for additional geometrical characteristics of
671 the solar panels, for example to better describe the effects of the secondary (transverse) slope when
672 it becomes of the same order as the tilting angle of the panels (i.e. their prevalent slope). This is the
673 typical case in which the secondary slope is prone to increase the heterogeneity of rain redistribution
674 by redistributing the collected water along the width of the panels. The presence and effect of a
675 ridge on the length and/or width of the panels could be explicitly modeled with the techniques used
676 in hydrology for thin flows over a weir. Even if the presence of a small ridge may affect the threshold
677 of (approximately) 2 mm water depth thought to trigger runoff on the panels (in controlled
678 conditions and without a ridge), it is hypothesized here that any explicit modelling would not provide
679 a significant added value, for two reasons: the stored volumetric amounts are small when the panels
680 are held nearly flat in absence of rain and the avoidance strategy is recommended when rain occurs.

Supprimé: weak

682 4.2. Rain redistribution in soils

683
684 Hydrus-2D was used to simulate rain redistribution in soils, using the spatially distributed output
685 variables of the AVrain model to provide the required time-variable atmospheric conditions. Five
686 such conditions at most can be used as climatic forcings for Hydrus-2D, which seemed a limitation for
687 the present purpose but could be handled, thus with the a posteriori indication that the chosen
688 "trick" has the value of a good practice. In coherence with the field observations, the simulated fields
689 of soil water content emphasized the interest of using the avoidance strategy to decrease the spatial
690 heterogeneities of soil water content in the agrivoltaic plots, confirming thus that the tilting angle of
691 the panels is a strong control parameter.

692
693 Even if the spatial heterogeneity of rain redistribution is less drastic in soils than on the soil surface,
694 due to lateral diffusion, it remains strong enough to necessitate a dedicated remediation in the form
695 of precision irrigation, unless the avoidance strategy is used. In other words the avoidance strategy
696 (that consists in minimizing rain interception and redistribution by commanding the appropriate
697 time-variable tilting angle of the panels) has implications in the relevant irrigation strategy, making it
698 less complex. This is an opening to a more global optimisation problem in dealing with the various

700 sources of heterogeneity, certainly to be compared with the observed heterogeneities in crop yield
701 on the agrivoltaic plots. Besides the heterogeneities in the forcings (irrigation and rain redistribution)
702 the modeller will surely have to also address these in soils, for example by means of geophysical
703 methods that offer the possibility of similar spatial resolutions (e.g., electrical resistivity tomography,
704 refraction seismology)

705

706 *4.3. Rain and crop-induced operation of solar panels*

707

708 Some aspects specific to cultivated plots need to be mentioned here, although the primary scope of
709 this paper is to focus on the hydrological side. The panels left with a low tilting angle (high surface
710 coverage and rain interception) are prone to have unwanted direct effects on the soil and plants
711 underneath. For example, leafy vegetables might be damaged by the repeated drop impacts or even
712 more by the occasional curtains of water falling from the panels a few meters above, even if their
713 storage capacity is limited. Such problems will typically occur in the morning, when panels are first
714 operated, being that they are generally left flat during nighttime. They could also occur during heavy
715 rains, even when using the avoidance strategy, which results in a damped but non-zero flux
716 concentration near the aplomb of the edges of the solar panels. In the bare soil periods, it is rather
717 the erosion risk that should be handled, especially "splash erosion" (Nearing and Bradford, 1985;
718 Josserand and Zaleski, 2003; Planchon and Mouche, 2010) where drop impacts are responsible for
719 particle detachment and for the creation of microtopography. This, in turn, creates pathways for
720 runoff and further soil degradation processes. Nevertheless, avoidance strategies fed by real-time
721 wind and precipitation data (collected at a 30 s time step) are powerful means to handle these
722 issues, certainly to be included in the more general optimisation strategies suitable for the cultivated
723 agrivoltaic plots. In some contexts, randomized positioning of the solar panels during rainfalls could
724 be another option to reduce the consequence of rain concentration on soil, and to maximize
725 homogeneity on the long term.

726

727

Supprimé: , which

Supprimé: s

730 5. Conclusion

731 Agrivoltaism represents a modern, relevant solution to the growing food and energy demands,
732 associated with a global population increase, especially in the current climate change context. But
733 still there are unresolved issues specific to the implementation of solar panels on the cultivated plots,
734 for example regarding the adaptation of the plants to the forced intermittent shading conditions, or
735 the impact of the panels on the hydrological budget and behavior of the plot. This paper has tackled
736 the pending question of rain redistribution by "dynamic" solar panels, i.e. panels endowed with one
737 degree of freedom in rotating around their supporting axis, so that their tilting angle may vary in time
738 and be controlled on purpose, on a very short term of a few minutes.

739 A dramatic difference was observed and simulated, in terms of spatial patterns of rain redistribution
740 on the ground, between the case of panels held flat and panels moved according to so-called
741 "avoidance strategies" that consist in minimizing rain interception by the panels during the course of
742 rain events (and eventually adapting the command of the panels to short-term changes in wind and
743 rain conditions within a single event). The avoidance strategies resulted in far lesser coefficients of
744 variation (i.e. heterogeneity measures) used to describe the spatial variations of the effective rain
745 amounts falling on the ground, under the panels, between panels, or near the aplomb of the edges of
746 the panels. The measures of heterogeneity obtained for avoidance strategies had low enough values
747 to be compared with the fairly good uniformity scores used to quantify the ability of irrigation
748 systems to deliver similar water amounts in the different zones of a given plot. Hence, it is likely that
749 the most relevant irrigation strategies will suppress or attenuate the need for precision irrigation
750 within the equipped plots. On the contrary, basic strategies that consist in holding the panels flat
751 induce very strong spatial heterogeneities, with local effective rain amounts that exceed these of the
752 control zone and may be responsible for increased runoff and erosion risks on bare soils, not to
753 mention the risks associated with direct, repeated impacts on the [soil aggregates \(possibly leading to](#)
754 [soil compaction and crust formation\) and on the](#) plants that find themselves near the aplomb of the
755 edge of the panels. The flat panel case has one additional disadvantage: the panels are never strictly
756 flat, so that any transverse slope of comparable order will have the consequence of redirecting all
757 the collected water towards a narrow outlet on the width of the panels.

758 However, the mechanistic AVrain model derived in this paper shows that the control exerted on the
759 tilting angle of the panels is strong enough for the user to cope with most meteorological conditions
760 (rain intensity, wind direction and velocity) and realistic structure characteristics (height, length and
761 spacing of the panels) to achieve the targeted short-term event-based optimisation of rain
762 redistribution. It is very likely that more general and complex methods should be used when
763 considering [at the same time](#) hydrological budget, crop growth and energy production, as well as
764 seasonal objectives. To prepare ground, the soil part of the problem has also been investigated here,
765 showing with Hydrus-2D simulations that rain redistribution patterns in soils resembled these
766 observed on the soil surface, though less contrasted due to lateral diffusion processes on the soil
767 surface (ponding) or within soils (at least where significant lateral dispersion coexists with gravity).
768 Future research leads include a finer parameterization of Hydrus-2D for a stronger coupling with the
769 results of the AVrain model, as a verification tool for the adaptation of simpler 1D approaches to
770 model water budget, irrigation strategies and crop growth in agrivoltaic conditions (Khaledian et al.,
771 2009; Mailhol et al., 2011; Cheviron et al., 2016) within global optimisation strategies.

772

773 **Code availability, data availability, sample availability**

774 Data collection and model development were performed in the frame of the Sun'Agri2B project that
775 links the Sun'R SAS society with Irstea and other academic or non-academic partners. The copyright
776 on all experimental and theoretical results presented here is governed by the consortium agreement
777 of the Sun'Agri2B project.

778

779 **Appendices and supplementary links**

780 None

781

782 **Team list**

783 The first author is a PhD student, member of both the Sun'R SAS society and the "OPTIMISTE"
784 research team of Irstea Montpellier, France, to which all co-authors also belong. OPTIMISTE stands
785 for Optimization of the Piloting and Technologies of Irrigation, Minimization of InputS, Transfers in
786 the Environment and is one of the research teams in the "G-Eau" joint research unit that addresses
787 water management, actors and usages.

788

789 **Author contribution**

790 Yassin Elamri performed most of the experiments and developed the model, under the supervision of
791 Bruno Cheviron and Gilles Belaud. Annabelle Mange contributed to the first stages of experiments
792 and model development while Cyril Dejean and François Liron helped handling the metrological and
793 technical parts of the work.

794

795 **Competing interests**

796 No known competing interests based on scientific grounds. However, there may be conflicts of
797 interest on commercial grounds with societies other than Sun'R SAS also engaged in agrivoltaic
798 activities.

799

800 **Disclaimer**

801 None

802

803 **Special issue statement**

804 None

805

806

807

808 **Acknowledgements**

809 This study was conducted within the frame of the SunAgri2b project, supported by Provence-Alpes-

810 Côte d'Azur and Rhône-Alpes Regions, CAPI, BPI France, Communauté de Communes Pays d'Aix,

811 Grand Lyon, the Agence Nationale pour la Recherche et la Technologie. The experimental platform

812 was co-funded by Irstea, Region Ile-de-France and Paris Entreprises.

813

814 **References**

- 815 ASAE. 1996. « Field evaluation of microirrigation systems ». *ASAE Standards. Amer. Soc. Agric. Engr.,*
816 *St. Joseph, MI., n° EP405.1:* 756-59.
- 817 Barakat, M., B. Cheviron, B. Deweppe, C. Dejean, L. Lassabaterre, and R. Angulo-Jaramillo. 2016.
818 « Numerical simulation of soil nitrate dynamics with Hydrus-2D for experimental maize plots
819 under sprinkler and subsurface drip irrigation ». *Agricultural Water Management* 178: 225-
820 38.
- 821 Barnard, T., M. Agnaou, and J. Barbis. 2017. « Two Dimensional Modeling to Simulate Stormwater
822 Flows at Photovoltaic Solar Energy Sites ». *Journal of Water Management Modeling.*
- 823 Best, A. C. 1950. « The Size Distribution of Raindrops ». *Quarterly Journal of the Royal Meteorological*
824 *Society* 76 (327): 16-36.
- 825 Burt, C. M., A. J. Clemmens, T. S. Strelkoff, K. H. Solomon, R. D. Bliesner, L. A. Hardy, T. A. Howell, and
826 D. E. Eisenhauer. 1997. « Irrigation Performance Measures: Efficiency and Uniformity ». *Journal of Irrigation and Drainage Engineering* 123 (6).
827
- 828 Campolongo, F., J. Cariboni, and A. Saltelli. 2007. « An Effective Screening Design for Sensitivity
829 Analysis of Large Models ». *Environmental Modelling & Software* 22 (10): 1509-18.
- 830 Cheviron, B., R. W. Vervoort, R. Albasha, R. Dairon, C. Le Priol, and J.C. Mailhol. 2016. « A Framework
831 to Use Crop Models for Multi-Objective Constrained Optimization of Irrigation Strategies ». *Environmental Modelling & Software* 86: 145-57.
832
- 833 Chow, V. **I.** 1959. *Open Channel Hydraulics*. McGraw-Hill Book Company.
- 834 Cook, L. M., and R. H. McCuen. 2013. « Hydrologic Response of Solar Farms ». *Journal of Hydrologic*
835 *Engineering* 18 (5): 536-41.
- 836 Delahaye, J.-Y., L. Barthès, P. Golé, J. Lavergnat, and J.P. Vinson. 2006. « A Dual-Beam
837 Spectropluviometer Concept ». *Journal of Hydrology* 328 (1-2): 110-20.
- 838 Diermanse, F.L.M. 1999. « Representation of Natural Heterogeneity in Rainfall-Runoff Models ». *Physics and Chemistry of the Earth, Part B: Hydrology, Oceans and Atmosphere* 24 (7): 787-
839 92.
840

841 Dinesh, H., and J. M. Pearce. 2016. « The Potential of Agrivoltaic Systems ». *Renewable and*
842 *Sustainable Energy Reviews* 54: 299-308.

843 Dupraz, C., H. Marrou, G. Talbot, L. Dufour, A. Nogier, and Y. Ferard. 2011. « Combining Solar
844 Photovoltaic Panels and Food Crops for Optimising Land Use: Towards New Agrivoltaic
845 Schemes ». *Renewable Energy* 36 (10): 2725-32.

846 Emmanuel, I., H. Andrieu, E. Leblois, N. Janey, and O. Payraastre. 2015. « Influence of Rainfall Spatial
847 Variability on Rainfall? Runoff Modelling: Benefit of a Simulation Approach? » *Journal of*
848 *Hydrology* 531: 337-48.

849 Faurès, J.-M., D.C. Goodrich, D. A. Woolhiser, and S. Sorooshian. 1995. « Impact of Small-Scale Spatial
850 Rainfall Variability on Runoff Modeling ». *Journal of Hydrology* 173 (1-4): 309-26.

851 Gumiere, S. J., Y. Le Bissonnais, and D. Raclot. 2009. « Soil Resistance to Interrill Erosion: Model
852 Parameterization and Sensitivity ». *CATENA* 77 (3): 274-84.

853 Gunn, R., and G. D. Kinzer. 1949. « The Terminal Velocity of Fall for Water Droplets in Stagnant Air ». *Journal of Meteorology* 6 (4): 243-48.

855 Harinarayana, T., and K. Sri Venkata Vasavi. 2014. « Solar Energy Generation Using Agriculture
856 Cultivated Lands ». *Smart Grid and Renewable Energy* 05 (02): 31-42.

857 IPCC. 2011. *Renewable Energy Sources and Climate Change Mitigation: Summary for Policymakers*
858 *and Technical Summary : Special Report of the Intergovernmental Panel on Climate Change.*
859 New York: Cambridge University Press.

860 IPCC. 2014. *Climate Change 2014: Impacts, Adaptation and Vulnerability. Contribution of Working*
861 *Group II to the Fifth Assessment Report of the Intergovernmental Panel on Climate Change.*
862 New York: Cambridge University Press.

863 Jackson, N.A. 2000. « Measured and Modelled Rainfall Interception Loss from an Agroforestry System
864 in Kenya ». *Agricultural and Forest Meteorology* 100 (4): 323-36.

865 Josserand, C., and S. Zaleski. 2003. « Droplet Splashing on a Thin Liquid Film ». *Physics of Fluids* 15 (6):
866 1650.

867 Khaledian, M.R., J.C. Mailhol, P. Ruelle, and P. Rosique. 2009. « Adapting PILOTE model for water and
868 yield management under direct seeding system: The case of corn and durum wheat in a
869 Mediterranean context ». *Agricultural Water Management* 96 (5): 757-70.

870 Knapen, A., J. Poesen, G. Govers, G. Gysels, and J. Nachtergaele. 2007. « Resistance of Soils to
871 Concentrated Flow Erosion: A Review ». *Earth-Science Reviews* 80 (1-2): 75-109.

872 Lamm, F. R., and H. L. Manges. 2000. « PARTITIONING OF SPRINKLER IRRIGATION WATER BY A CORN
873 CANOPY ». *Transactions of the ASAE* 43 (4): 909-18.

874 Levia, D. F., and S. Germer. 2015. « A Review of Stemflow Generation Dynamics and Stemflow-
875 Environment Interactions in Forests and Shrublands: STEMFLOW REVIEW ». *Reviews of*
876 *Geophysics* 53 (3): 673-714.

877 Mailhol, J.C., P. Ruelle, S. Walsler, N. Schütze, and C. Dejean. 2011. « Analysis of AET and yield
878 predictions under surface and buried drip irrigation systems using the Crop Model PILOTE
879 and Hydrus-2D ». *Agricultural Water Management* 98 (6): 1033-44.

880 Marrou, H. 2012. « Produire des aliments ou de l'énergie: faut-il vraiment choisir? - Evaluation
881 agronomique du concept d'"agrivoltaïsme" ». Montpellier: Montpellier Sup'Agro.

882 Marrou, H., L. Dufour, and J. Wery. 2013a. « How Does a Shelter of Solar Panels Influence Water
883 Flows in a Soil-crop System? » *European Journal of Agronomy* 50: 38-51.

884 Marrou, H., L. Guilioni, L. Dufour, C. Dupraz, and J. Wery. 2013b. « Microclimate under Agrivoltaic
885 Systems: Is Crop Growth Rate Affected in the Partial Shade of Solar Panels? » *Agricultural*
886 *and Forest Meteorology* 177: 117-32.

887 Marrou, H., J. Wery, L. Dufour, and C. Dupraz. 2013c. « Productivity and Radiation Use Efficiency of
888 Lettuces Grown in the Partial Shade of Photovoltaic Panels ». *European Journal of Agronomy*
889 44: 54-66.

890 Martello, M., N. Ferro, L. Bortolini, and F. Morari. 2015. « Effect of Incident Rainfall Redistribution by
891 Maize Canopy on Soil Moisture at the Crop Row Scale ». *Water* 7 (5): 2254-71.

892 Morris, M. D. 1991. « Factorial Sampling Plans for Preliminary Computational Experiments ». *Technometrics* 33 (2): 161.

893

894 Movellan, J. 2013. « Japan Next-Generation Farmers Cultivate Crops and Solar Energy ». *Renewable*
895 *Energy World*. [http://www.renewableenergyworld.com/articles/2013/10/japan-next-](http://www.renewableenergyworld.com/articles/2013/10/japan-next-generation-farmers-cultivate-agriculture-and-solar-energy.html)
896 [generation-farmers-cultivate-agriculture-and-solar-energy.html](http://www.renewableenergyworld.com/articles/2013/10/japan-next-generation-farmers-cultivate-agriculture-and-solar-energy.html).

897 Nearing, M. A., and J. M. Bradford. 1985. « Single Waterdrop Splash Detachment and Mechanical
898 Properties of Soils¹ ». *Soil Science Society of America Journal* 49 (3): 547.

899 Niu, S., X. Jia, J. Sang, X. Liu, C. Lu, and Y. Liu. 2010. « Distributions of Raindrop Sizes and Fall
900 Velocities in a Semiarid Plateau Climate: Convective versus Stratiform Rains ». *Journal of*
901 *Applied Meteorology and Climatology* 49 (4): 632-45.

902 Osborne, M. 2016. « Fraunhofer ISE resurrects agrophotovoltaics ». *PVTECH*. [http://www.pv-](http://www.pv-tech.org/news/fraunhofer-ise-resurrects-agrophotovoltaics)
903 [tech.org/news/fraunhofer-ise-resurrects-agrophotovoltaics](http://www.pv-tech.org/news/fraunhofer-ise-resurrects-agrophotovoltaics).

904 Pereira, L. S., T. Oweis, and A. Zairi. 2002. « Irrigation Management under Water Scarcity ».
905 *Agricultural Water Management* 57 (3): 175-206.

906 Planchon, O., and E. Mouche. 2010. « A Physical Model for the Action of Raindrop Erosion on Soil
907 Microtopography ». *Soil Science Society of America Journal* 74 (4): 1092.

908 Playán, E., and L. Mateos. 2006. « Modernization and Optimization of Irrigation Systems to Increase
909 Water Productivity ». *Agricultural Water Management* 80 (1-3): 100-116.

910 Pujol, G., B. looss, and A. Janon. 2017. *Global Sensitivity Analysis of Model Outputs* (version 1.14.0).
911 Package « sensitivity ».

912 Ravi, S., D. B. Lobell, and C. B. Field. 2014. « Tradeoffs and Synergies between Biofuel Production and
913 Large Solar Infrastructure in Deserts ». *Environmental Science & Technology* 48 (5): 3021-30.

914 Simunek, J., M. Sejna, and M. Th. van Genuchten. 1999. « The HYDRUS-2D Software Package for
915 Simulating the Two-Dimensional Movement of Water, Heat, and Multiple Solutes in
916 Variably-Saturated Media (Version 2.0) ». Riverside, California: U.S. SALINITY LABORATORY,
917 AGRICULTURAL RESEARCH SERVICE, U.S. DEPARTMENT OF AGRICULTURE.

918 Tang, Q., T. Oki, S. Kanae, and H. Hu. 2007. « The Influence of Precipitation Variability and Partial
919 Irrigation within Grid Cells on a Hydrological Simulation ». *Journal of Hydrometeorology* 8 (3):
920 499-512.

921 Van Hamme, T. 1992. « La pluie et le topoclimat ». *Hydrologie Continentale* 7 (1): 51-73.

- 922 [Van der Gulik, T., S. Tam et A. Petersen. 2014. "B.C. Sprinkler Irrigation Manual". Prepared by the B.C.](#)
923 [Ministry of Agriculture and Fisheries. Irrigation Industry Association. B.C., Canada.](#)
- 924 Yuan, C., G. Gao, and B. Fu. 2017. « Comparisons of Stemflow and Its Bio-/Abiotic Influential Factors
925 between Two Xerophytic Shrub Species ». *Hydrology and Earth System Sciences* 21 (3): 1421-
926 38.